International Journal of Innovative Technology and Exploring Engineering (IJITEE)
ISSN: 2278-3075 (Online), Volume-8 Issue-12, October 2019

# Photocatalytic Degradation of Allura Red by Mn-Ni co-doped Nanotitania under Visible Light Irradiation

**Sankara Rao Miditana, Siva Rao Tirukkovalluri, Shaik Abdul Alim, Imandi Manga Raju**

***Abstract:*** ***Photocatalyst has been extensive interest because of it's new innovation to the reduce the contamination in the environment. A straight forward and economical procedure has been employed by sol-gel technique for the co-doping of $Mn^{2+}$ and $Ni^{2+}$ into $TiO_2$. The co-doped and undoped photocatalysts were described by X-ray diffraction (XRD), Scanning electron microscopy (SEM), Energy dispersive X-ray Spectroscopy (EDX), Fourier transform infrared spectroscopy (FT-IR), UV-Visible Diffused Reflectance Spectroscopy (UV Vis-DRS), Transmission electron Microscopy (TEM) and Brunauer-Emmett-Teller (BET). The portrayal results shows that anatase and rutile mixed phase was observed for some co-doped nanocatalysts and the remaining catalysts exhibits anatase phase only. It was observed by FT-IR that the shifting of frequency of Ti-O-Ti in the catalysts was seen due to substitutional doping of Mn and Ni by replace Ti and O, further the photocatalysts shows rough morphology, irregular shape of particle with size (6.5nm) and having high surface area (135.70 $m^2$/g), less band energy (2.7 eV). The photocatalytic action of these materials was assessed by the degradation of Allura red (AR) as a contaminant. The results shows that AR has degraded within 60 minutes at doping concentrations 0.25 Wt% of $Mn^{2+}$ ion and 1.0 Wt% of $Ni^{2+}$ ion in $TiO_2$ (NMT2) at an optimum reaction parameters pH-4, catalyst dose 0.070g/L and at AR initial dye concentration 0.010g/L.***

***Keywords: Manganese, Nickel, Allura red, Photocatalysis, Sol-gel mehtod, co-doping, $TiO_2$***

## I. INTRODUTION

The best compound materials gathering delivered on the planet is painting, pulp and textile ventures. During the processes of such industries pollutants enter to nature [1]. In this manner, material and painting businesses contaminations are a fundamental wellspring of the ecological natural defilements, so removal and transformation of them into innocuous mineral mixes is a significant issue. Then again, material and painting ventures are the most expending of water. Accordingly, in these ventures a lot of wastewater is coming out during different processes of industries.

**Revised Manuscript Received on October 30, 2019.**
***** Correspondence Author
**Mr. Sankara Rao Miditana***, Lecturer in Chemistry at STSN Government Degree College, Kadiri, Andhra Pradesh, India.
**Prof. T. Siva Rao**, Professor and Research Director, Dept. of Inorganic & Analytical Chemistry, A.U. College of Science & Technology, Andhra University, Visakhapatanam, A.P, India.
**Dr. Shaik Abdul Alim**, Ph.D. A.U. College of Science & Technology, Andhra University, Visakhapatanam, A.P, India.
**Mr. Imandi Manga Raju**, M.Sc, A.U. College of Science & Technology, Andhra University, Visakhapatanam, A.P, India.



On the off chance that wastewater without purification enters to the earth, it tends to be influence water biological system with a wide range of techniques. Without a doubt, painting and its deterioration could be a noteworthy danger to the earth [2, 3]. So that, purification of wastewater is extremely fundamental before it is released to nature.

Different kind of physical and chemical techniques are utilized for this reason most significant of them is including; adsorption, reverse osmosis and precipitation methods.

These techniques just change the phase of contamination and they are focus on non-damaging procedures. In the current days water can be purified by the advance oxidation process (AOP). In this procedure, free hydroxyl radicals are utilized for debasement of contamination and transformation to innocuous mineral materials, for example, carbon dioxide, water, and mineral salts [4]. Disintegration of the intensity 0f photocatalyst by utilizing titanium dioxide nanocatalyst go with UV light is among AOP that its utilization will extent [5]. Fundamental parameter for a semiconductor photocatalyst is that decrease the e-/h+ recombination in such way reduce the bandgap of semiconductor. Reduction ability of photo electrons by the low conduction band and the high level conduction band reduce the holes produced by the light. Notwithstanding appropriate energy bandgap for a semiconductor, it must be easy to produce, low cost, harmless for human beings and nature.

Heterogeneous photocatalytic oxidation utilizing semiconductors is a considerable method for air and water decontamination. $TiO^2$ is commonly acknowledged as one of the best photocatalyst and is regularly used to oxidize organic compounds in air and water because of its oxidative capacity and photo stability. $TiO^2$ is likewise a typical, non-costly and non-dangerous material [6]. Three crystalline structures are possible to the $TiO^2$; anatase, rutile and brookite. Anatase and rutile have a place with the huge bandgap semiconductors with bandgap energies of 3.2 and 3.0 eV separately [6]. Anatase is fundamentally the polymorph phase which has generally been utilized in photocatalytic process for de-contamination purposes. Compared to pure anatase or rutile, mixed phase of anatase and rutile is photocatalytically active [7]. Many researchers solved the problem by the doping of metalions [8] an ideal concentration of the dopants favored to control the crystallite size of nano doped $TiO^2$, reducing the bandgap favours to form high surface area [9]. As per the reports of literature survey represented that the doping of transition metal like Mn and Ni [10] into $TiO^2$ causes contortion of precious electronic structure because of collaboration of d-orbitals of doped change metal particles with Ti-3d orbital lower level of the conduction band and lessen the bandgap [11].

During the irradiation, metals also reduce the e-/h+ recombination. The metal doped $TiO^2$ was acquired by dispersal of metal nanoparticles into $TiO^2$ framework. An affixed advantage of metal doping like Mn, Cr, Ni, Cu [12-13] were improved the catching of electron to hinder the e-/h+ recombination during radiation of light.

In the present examination, Nickel and Manganese transition metals were selected for the synthesis of Mn-Ni co-doped $TiO^2$ by using sol-gel method. Presence of t2g orbital of d of these metals is very close to conduction band that's why these metals are preferred [11, 14].

In the visible region Manganese has the best potential in allowing optical absorption, through this narrow the bandgap [11]. In the Mn-Ni co-doped $TiO^2$ $Mn^2$+ and $Ni^2$+ ions are easily replace the $Ti^4$+ in $TiO^2$ lattice because ionic radii of $Ti^4$+ (0.068nm) is similar with ionic radii's of $Mn^2$+ ( 0.078nm) and $Ni^2$+(0.072nm) [15]. On other hand, the presence of Ni particles in $TiO^2$ lattice can frame heterojunctions between n-type $TiO^2$ and p-type Ni oxide dopant. These p-n junctions are useful to separation of electron-hole through the electric field and encourage the interfacial charge move [16]. There exist different techniques for synthesis of titania nanoparticles like sol-gel process, electrochemical method, flame aerosol process, micro emulsion method, thermolysis, chemical vapor deposition, etc. [17]. Among every one of these techniques sol-gel strategy is frequently utilized and it offers the points of interest, exact command over the stoichiometry, low temperature preparation, high crystallinity and high immaculateness [18].

As prepared samples were tested for its photocatalytic capability by utilizing a model dye pollutant Allura Red (AR). AR is mostly used as coloring agent in food industry. Oxidizing and decreasing agents present in nourishments such as sugars, acids and salts, lead to some precariousness of the Allura red color, since coloring properties depends on the conjugated unsaturated framework of a molecule.

It has adverse toxic effects in reproductive system and neurobehavioral nature in animals and humans. And it is hypersensitive to asthma and skin rashes [19].

## II. EXPERIMENTAL PART

### A. Materials used :

Chemicals used in this method were reagent grade and used without any further purification. N-butyl tetra orthotitanate ($Ti(OBu)_4$), Manganese nitrate $[Mn(NO_3)_2].6H_2O$ and Nickel nitrate $[Ni(NO_3)_2].6H_2O$ were acquired from E-Merck Germany and used as a precursors for Titanium, Manganese and Nickel for getting ready undoped $TiO_2$ and co-doped $TiO_2$ nanoparticles separately. Allura red pollutant was used as a model pollutant from High media, India.

### B. Synthesis of nanocatalyst :

By using sol-gel technique Manganese and Nickel co-doped nanotitania was prepared [20-21]. In this procedure n-Butyl orthotitanate (20mL) was added to 40 ml of ethanol and acidified with 3.2 ml of $HNO_3$ taken in a 150 ml pyrex glass measuring beaker (Solution-A) and then stirred for 15min. Mn and Ni dopent weights according to titania weight percentage were taken in another beaker and then add 40 ml of ethanol and after that 7.2 ml of 2D water to effective hydrolysis process (Solution-B). Now mix the solution-B to solution-A slowly in dropwise manner with continuous stirring. After completion of mixing of solution-B sol was obtained on further vigorous stirring for 90 min and keeps mixing for 90 min and aged for 48h then form gel. The formed gel was dried at 70 $^oC$ and grounded it and calcined at 430 $^oC$ for about 5h in furnace. At long last homogeneous powder was obtained. Prepare the undoped $TiO_2$ in absence of dopants (Mn and Ni). Different weight percentages (0.25 Wt% - 1.0 Wt%) of Mn and Ni co-doped nanocatalysts synthesized by using above said procedure. Weight percentages of Mn and Ni are shown in Table 1.

Table.1: Name assigned to different of co-doped $TiO_2$ catalyst samples

| S.No | Dopant (Transition metal) weight percentages in $TiO_2$ (Wt%) | Name assigned to co-doped $TiO_2$ Catalyst |
|---|---|---|
| **1** | 1.00 Mn 0.25 Ni | NMT1 |
| **2** | 0.25 Mn 1.00 Ni | NMT2 |
| **3** | 0.50 Mn 0.50 Ni | NMT3 |
| **4** | 0.25 Mn 0.75 Ni | NMT4 |
| **5** | 0.75 Mn 0.25 Ni | NMT5 |
| **6** | Nil | undoped $TiO_2$ |

### C. Experimental techniques used for characterization of the catalysts :

The crystalline structure of photocatalysts were detected by powder X-ray diffraction (XRD) spectra taken (PAN Analytical) utilizing anode Cu-WL 1 ($\lambda$=1.5406nm) radiation with a nickel channel. 40 mA and 40 kV were applied current and voltage respectively. Basing on the Scherrer equation using full width at half maximum (FWHM) crystallite size of anatase was predicted. The surface area and porosity of nanocatalysts were completed with a micrometrics Gemini VII surface area analyzer. The $N_2$ adsorption/desorption isotherms were recorded and noted by BJH surface/volume meso pore technique. By using Frenkel-Halsey-Hill isotherm equation pore volume was determined. Every catalyst was degassed at $300^0C$ for 2 h. The size and geometry of samples were recorded with TEM utilizing JEOL/JEM 2100, worked at 200 kV. By the scanning electron microscopy (SEM) (ZEISS-SUPRA 55 VP) with energy dispersive X-beam (EDS) spectrophotometer, morphology and elemental composition of samples were predicted. FT-IR spectra of the nanocatalysts were recorded on a FT-IR spectrometer (Nicolet Avatar360). The Diffuse reflectance spectra (DRS) of the catalysts were recorded in the range of 200-900 nm with a Shimadzu 3600 UV-Visible-DRS Spectrophotometer using $BaSO_4$ as reference. The photocatalytic activity of AR dye was observed by the UV-Vis spectrophotometer (Shimadzu1601).

### D. Experimental procedure to the determination of catalytic activity of nanocatalyst:

Efficiency of Mn-Ni co-doped nanocatalyst was determined by the degradation of AR pollutant under visible region [22]. Pressure of 400W (35,000 lm) mercury vapor light with UV filter (Oriel, 51472) was utilized as a noticeable light source.

The total degradation was processed by taking 100 mL of AR solution of particular concentration (1-10 $mgL^{-1}$) containing adequate measure of the impetus in a 150 mL Pyrex glass vessel under vigorous stirring put around 20 cm away from the light source.

The running water was flowed around the nanocatalyst container to IR radiation and furthermore to keep up consistent solution temperature in the reaction. Before going to expose to radiation the dye solution stirred for 30 min in dark condition to adsorption – desorption equilibrium of AR on the surface of the catalyst.

After exposed to visible light 5 ml of aliquots tests were collected at various interims of time to watch the intensity of AR at 540 nm utilizing UV-vis Spectrophotometer. To observe the pH effect of solution pH meter (Elico Digital pH meter model 111E, EI) was used at the time of degradation process. To get required pH add 0.1 N NaOH/ 0.1 N HCl basing on the nature of testing solution. The percentage of degradation of AR pollutant was determined by the following formula [21].

$$\% \text{ of Degradation} = A0 - At/A0 \times 100$$

Where, A0 is starting absorbance of dye solution before debasement and At is absorbance at time t. The ideal conditions are achieved by differing the parameters of reaction like concentration of dopant, pH effect, dosage of catalyst and initial dye concentration and obtained results are discussed in section. IV.

## III. RESULTS AND DISCUSSION

### A. X-ray Diffraction study (XRD):

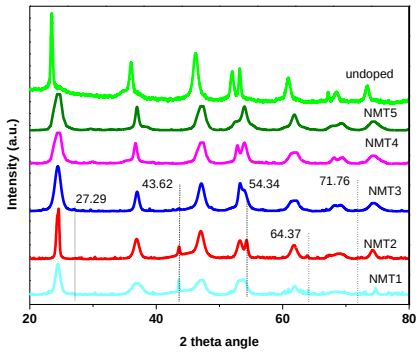


**Fig.1. XRD patterns of undoped and co-doped NMT catalysts**

Structural properties and crystallinity of Manganese and Nickel co-doped $TiO_2$ of various phases in XRD of nanocatalysts after calcination at 450 $^0$C was shown in Fig.1. All diffraction lines are generally rigid, which showing a high crystallinity for prepared catalysts. From the diffraction data it is found that anatase and rutile mixed phase is observed for NMT1, NMT2, NMT3 catalysts. The anatase stage was affirmed with the Joint Committee on Powder Diffraction Standard (JCPDS) record no. 21- 1272. Peaks are find at 2θ= 25.28, 37.81, and 48.05 related to the (101), (004), and (200) planes of anatase. While the peaks at 2θ= 27.29, 44.10 and 54.32, related to the (110), (101) and (220) planes of rutile structure with the JCPDS document no. 21-1276 [23]. The presence of rutile in the nanomaterial was promptly perceivable from its (110) diffraction pinnacle situated at 2 theta of 27.29° in the XRD pattern, due to no overlapping of this peak with any other peak from anatase obtained. Anatase phase can be effectively recognized from its (101) peak situated at 2 theta of 25.3°, as this pinnacle doesn't cover with some other peaks of rutile. This outcome obviously shows that rutile and anatase coincided in the examples NMT1-NMT3. Further NMT4, NMT5 and undoped $TiO^2$ indicates anatase phase as it were. The crystallite sizes of prepared catalysts were predicted by the Debye–Scherrer equation by utilizing large intensity of anatase (101) and rutile (110) diffraction peaks, the outcomes were appeared in Table 3.

### B. Scanning electron Microscopy & Energy dispersive Spectroscopy (SEM-EDX):

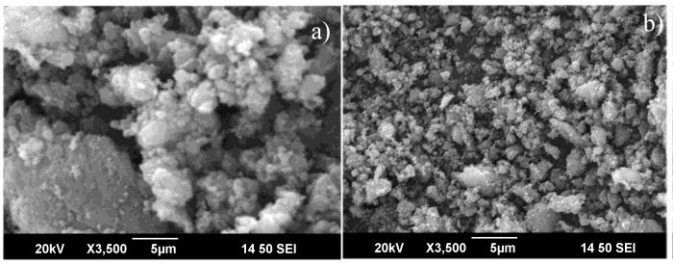


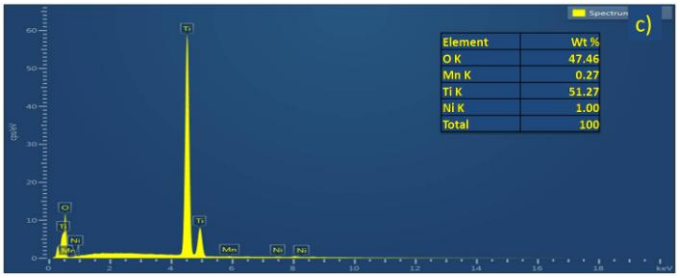


**Fig.2. Sem images of a) undoped $TiO_2$ and b) NMT2 c) EDX spectra of NMT2**

The morphology and size of the nanocatalyst assume significant job in its photocatalytic movement [20] and were tested by the SEM. Fig.2 shows that the SEM micrograph of the as prepared undoped $TiO_2$ and NMT2 nanocatalysts. In the Fig.2 (a) undoped $TiO_2$ clearly revealed large particle size and Fig. 2(b) co-doped $TiO_2$ shows small particle size, which leads to high surface area, correlated with BET results. The morphology has different shapes of grains with irregular boundaries. Pictures of undoped $TiO_2$ (Fig.2(a)) show irregular shapes and amassed particles. HRSEM of 1.00 wt% of Ni and 0.25 wt% of Mn–$TiO^2$ (Fig. 2(b)) indicates less agglomeration and dispersive nature when compared to undoped and rest of samples. SEM pictures reveals that due to codoping agglomeration was considerably diminished. The elemental composition of samples predicted by EDS detector, which was connected to a SEM appeared in Fig.2c. EDX investigation shows that the elements of Ti, O, Ni and Mn are present in the sample.

### C. Transmission electron microscopy (TEM):

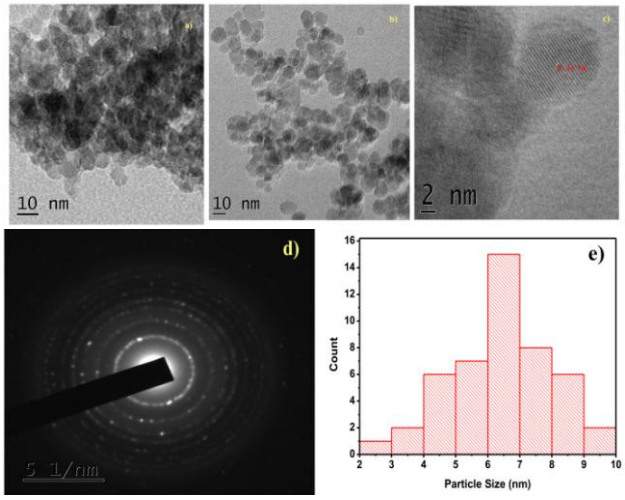


**Fig. 3. TEM images of a) undoped $TiO_2$ and b) NMT2 c) NMT2 showing lattice fringes. d) SAED pattern of NMT2 e) NMT2 particle size distribution.**

From the TEM images it was obtained that size distribution of particle by measuring the diameter of particles. The TEM micrographs of undoped and co-doped (NMT2) $TiO_2$ catalysts are appeared in Fig.3 (a) and (b). From the pictures it is seen that the molecule size of NMT2 is littler size when compared with undoped $TiO_2$. The Fig.3c demonstrates that catalyst particles lattice fringes with d spacing 0.33 nm related to 101 plane of anatase phase of $TiO_2$. SAED pattern indicates the no change is observed in structural arrangement of anatase $TiO_2$ (Fig. 3d) and the planes are (101), (004), (200) and (211). Fig.3(e) demonstrates that the average size of the nanocatalyst is 6.5 nm, which was compute from Gaussian fitting of the size Histogram [24-25]. These outcomes affirmed that the co-doping of Ni and Mn lessens the molecule size of $TiO_2$.

### D. Fourier Transform –Infra Red Spectroscopy (FT-IR):

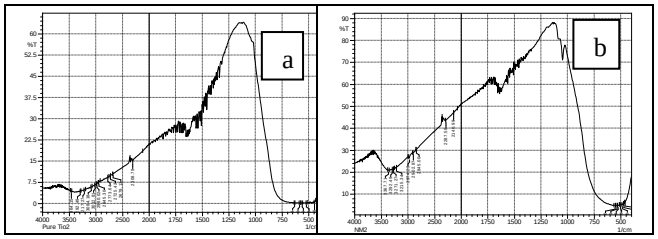


**Fig.4. FTIR spectra of a) undoped $TiO_2$ b) NMT2**

Undoped and $Ni^{2+}$, $Mn^{2+}$co-doped $TiO_2$ nano materials were identified by FT-IR spectra and were shown in Fig.4. The obtained peaks at 3012 $cm^{-1}$ 3464 $cm^{-1}$, 1620 $cm^{-1}$ – 1635 $cm^{-1}$ [26] relating to extending vibrations of OH has a place with Ti-OH surface and bending vibrations of adsorbed H-OH. The solid assimilation band around 569 $cm^{-1}$ is because of extending vibrations of Ti-O-Ti and Ti-O band in undoped $TiO_2$ which is in great concurrence with past examinations [27]. From Fig.4a it is seen that in the wake of co-doping of Ni and Mn into $TiO_2$ the stretching vibrations of skeletal Ti-O-Ti moved to 569 $cm^{-1}$ to 605 $cm^{-1}$ demonstrated that Ni and Mn co-doped into $TiO_2$ by substituting Ti [28]. Further, there is appearance of the band located at 1020 $cm^{-1}$ for co-doped $TiO_2$ indicated that Ni and Mn are co-doped into $TiO_2$ lattice.

### E. Ultraviolet-Visible Diffuse Reflectance Spectroscopic studies (UV-Vis-DRS)

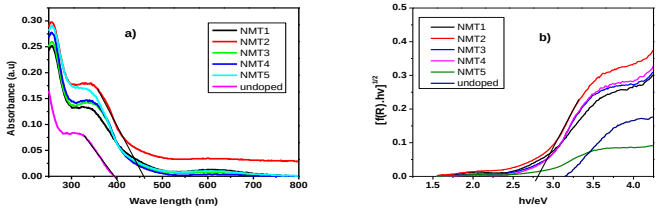


**Fig. 5. (a) The DRS spectra of undoped and co-doped $TiO_2$ with different weight % of Mn and Ni (b) Tauc plots of the square root of the Kubelka-Munk function determining band gap energy values.**

DRS spectral data of undoped and Ni, Mn co-doped $TiO_2$ nanocatalysts were shown in Fig.5, which shows that the assimilation of the electromagnetic spectra showed up at the visible region at around (400 nm–800 nm). NMTs (Ni and Mn) co-doped nanocatalysts gave the remarkable results in the bandgap and expansion of absorption edge towards Visible light wave length. This is might be because of the arrangement of an additional energy level over the valance band by Ni 2p narrowing the bandgap of $TiO_2$ [29]. This move is related with the doping just as the arrangement of stable rutile period of $TiO_2$ as represented in XRD. The inalienable explanation behind red shift in the bandgap is because of the difference in the sp-d cooperation between the band electrons and the restricted d-electrons of the $Ni^{2+}$ particles [30].

The manganese particle joined into $TiO_2$ crystal and it contorts the encompassing condition which impacts the conduction band of $TiO_2$ through the collaboration with Ti-3d orbitals which encourage to restrict the recombination of electron-hole pairs and broadened the optical reaction vitality [31]. Further it was bolstered by the determined bandgap energies of all the samples from the reflectance spectra utilizing the Kubelka-Monk formalism and Tauc plot strategy [32] appeared in Fig. 5(b). The undoped $TiO_2$ displayed the bandgap of 3.2 eV which is similar with the literature value [33] and the co-doped $TiO_2$ catalysts gave the bandgap values from 2.7 to 3.01 eV. Among all the co-doped tests NMT2 showing less bandgap (2.70 eV). In this way the outcomes demonstrated that all the co-doped catalysts are visible active and increase the photocatalytic degradation because of increasingly number of electron/hole pairs. Further, when thought about the bandgap values of Mn and Ni single doped $TiO_2$ impetuses (which are gotten from literature) the bandgap of NMT2 catalyst is reduced and the values are shown in Table.2 [34-35].

**Table: 2. The comparative band gap values of Mn and Ni single doped and Mn and Ni co-doped $TiO_2$**

| S.No | Doping elements | Catalysts Band gap energy (eV) | Reference No. |
|---|---|---|---|
| 1 | Mn | 2.95 | 28 |
| 2 | Ni | 2.99 | 29 |
| 3 | Undoped $TiO_2$ | 3.2 | 27 |
| 4 | Mn and Ni | 2.70 | Present work |

### F. Brauner-Emmett-Teller (BET)

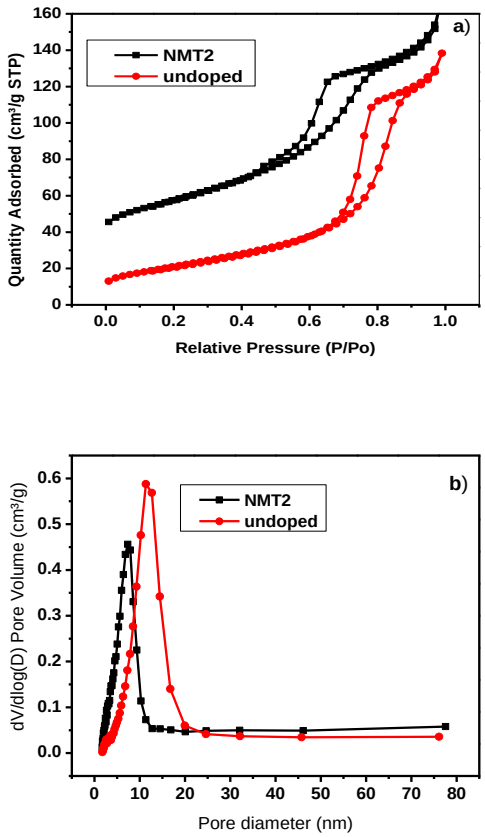


**Fig.6. (a) The $N_2$ adsorption–desorption isotherms and (b) pore diameter distribution curves of NMT2 co-doped $TiO_2$**

The particular surface area and porosity of the undoped $TiO_2$ and NMT2 were determined by utilizing the $N_2$ adsorption and desorption isotherms as appeared in Fig. 6a. Every one of the isotherms of synthesized samples indicates the stepwise adsorption and desorption part of type IV curves, demonstrating the mesoporous material having a three dimensional (3D) intersection as per the IUPAC order. A hysteresis loop with a stepwise adsorption and desorption branch is seen at wide range of pressure (P/Po), and the surface area of NMT2 mesoporous $TiO_2$ calcined at 450 $^0$C is 135.70 $m^2$/g as appeared in Fig.6a. The undoped $TiO_2$ surface area is 64 $m^2$/g as appeared in Fig.6a. This outcome shows that the material has more extensive mesoporous structure. To examination pore size and pore volume, the plots of the pore size appropriation are explored by desorption part of the BJH technique as appeared in Fig. 6b. The average pore diameter of mesoporous $TiO_2$ calcined at 450 $^0$C is 6.2 nm with moderately thin pore size distribution. The pore volume of mesoporous $TiO_2$ is 0.22 $cm^3$/g. Be that as it may, for undoped $TiO_2$ 10 nm pore size appropriation is observed and 0.21 $cm^3$/g pore volume also considered. Such a physical properties of huge surface area and high crystallinity with nano crystalline collected is great material for high photocatalytic action. This expanded surface zone may favors the adsorption of the more number of color particles on the outside of the impetus and it increases the degradation strength of the impetus.

**Table 3:** The Results of crystallite size (XRD), Band gap (UV-Vis- DRS) & BET surface area.

| S.No | Catalyst | Crystallite size (nm) | Band gap Energy (eV) | BET surface area analysis | | |
|---|---|---|---|---|---|---|
| | | | | Surface area ($m^2$/g) | Pore Volume ($cm^3$/g) | Pore Size (nm) |
| 1 | NMT1 | 7.35 | 2.74 | 113.41 | 0.22 | 7.3 |
| 2 | NMT2 | 6.5 | 2.70 | 135.70 | 0.22 | 6.2 |
| 3 | NMT3 | 7.31 | 2.78 | 114.06 | 0.22 | 7.3 |
| 4 | NMT4 | 7.9 | 2.84 | 106.81 | 0.20 | 8.2 |
| 5 | NMT5 | 8.50 | 3.0 | 88.87 | 0.20 | 9.3 |
| 6 | Un doped | 18.3 | 3.20 | 64.09 | 0.21 | 10 |

## IV. Assessment of Photocatalytic effect of NMT2 catalyst by degradation of Allura Red (AR) dye:

To set up the ideal parameters for effective photocatalytic debasement of AR pollutant with NMT2 impetus the experiments were processed under visible light illumination. At 540 nm measure the degradation rate at different intervals. Initially the degradation process takes place in absence of light for 60 minutes to a particular amount of dye solution. Then after catalyst was added to the dye solution and exposed to visible light. These results reveals that in the absence of light the pollutant particles adsorbed to the surface of the catalyst and then when exposed to the visible light adsorbed molecules to surface are degraded. In visible light these adsorbed molecules are gets degraded due to activation of the catalyst particles by expose of visible light. Therefore the absorption of dye was diminished. This is clear evidence that light and nanocatalyst are responsible to complete degradation of dye. Not only these two parameters effect the degradation of dye but also other parameters like dopant concentration, pH effect, catalyst dosage and initial dye concentration are degraded the dye solution. Experiments carried out by varying the one of the above parameters and rest of parameters kept constant.

### A. Effect of Dopant Concentration:

The impact of dopant concentration of undoped and Ni, Mn co-doped $TiO_2$ nanocatalysts were studied for photocatalytic effect for debasement of AR at 20 mg/L, impetus dosage 0.080 g/L and pH-3. The experimental values were drawn in Fig.7. From the figure all the co-doped catalysts shows preferred photocatalytic activity over that of undoped $TiO_2$ in visible region. Compared to other catalysts NMT2 exhibits better photocatalytic activity.

This is mainly due to the NMT2 having optimum parameters like high surface area, smaller in size.

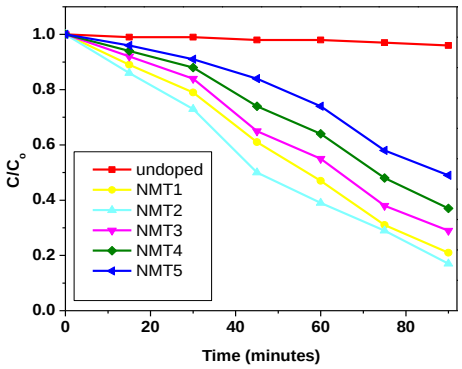


**Fig.7. Effect of dopant concentration on photocatalytic of co-doped nanoitania for rate of degradation of AR dye. Here, catalyst dosage 0.080 g/L, pH-3 and [AR]= 20 mg/L**

**B. Effect of pH:**

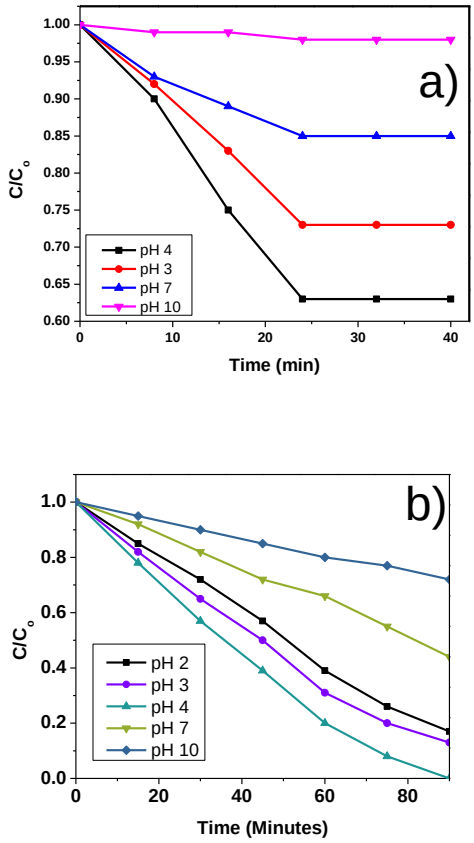


**Fig.8. a) Effect of pH in dark condition on the adsorption of AR dye, here NMT2 Catalyst dosage 0.080 g/L, dye 20 mg/L b)The effect of catalyst dosage on the degradation of AR dye, here NMT2 catalyst dosage 0.080 g/L and dye 20 mg/L.**

Effect of pH is plays significant role in the assessment of photocatalytic debasement of the impetus in aqueous medium. So as to investigate the impact of pH on the impetus surface dull responses were led without pH and with pH at 3, 4, 7 and 10.5 mL of aliquots were collected to every 10 min stirring and absorbance of solution of dye was estimated at 540 nm.From Fig. 8a at pH-4 the rate of adsorption of pollutant particles were expanded up to 24 min and later it become steady, this shows the color atoms are adsorbed on the surface of the impetus in a solitary layer, after that the adsorption may not occur. At pH-4 the adsorption of color atoms is extremely high. From Fig. 8a at pH-2 the adsorption diminishes contrasted with pH-4 and no adsorption was seen at pH-10 (Fig.8a). At pH-4 the rate of adsorption is extremely high. This is due to in dark condition pH of the sample solution was adjusted by the addition of 0.1 M HCl and then stir for 15 min and then after mix the dye solution with sample solution. By the addition of HCl solution the total surface of nanocatalyst make as positive, which is favorable to the interaction with the negative poles of dye particles [36] the adsorption is exceptionally high at pH-4 up to 24 min. in this way effect of pH can be examined by differing the pH from pH-2 to pH-10 as the adsorption of the color on the impetus surface is relies upon the pH [37] and remaining parameters kept constant at impetus dosage 0.080 g/L and 20 $mgL^{-1}$ is taken as initial dye concentration with NMT2 impetus. The test results showed in Fig.8b reveals that at pH-4 AR gives best photocatalytic degradation rate. At pH-4 large number of $H^+$ radicals are accessible which can replacethe OH of the M-OH groups and then surface area of nanocatalyst becomes more +Ve [38].

$$TiOH + H^+ \rightarrow TiOH_2 pH < 6.25$$

$$TiOH \rightarrow TiO^- + H^+ pH > 6.25$$

The presence of OH groups on the surface of the catalyst characterized by FT-IR OH stretching frequencies. Once the surface of the catalyst becomes +Ve (at pH-4) the –Ve dye molecules are electro statically interacted with +Ve surface of the catalyst [39] and facilitate the reaction between hydroxyl group, which produces at surface of the catalyst and adsorbed dye molecules. Hence, the rate of degradation increases.

**C. Effect of catalyst dosage:**

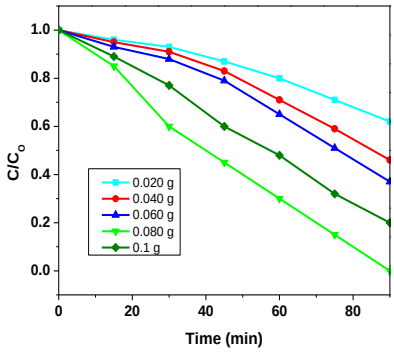


**Fig.9. Effect of NMT2 catalyst dosage, here pH-4 and AR concentration 20 $mgL^{-1}$**

Examine the catalyst at different catalyst dosage from 0.020 g/L to 0.1 g/L at constant pH-4 and the concentration dye 20 $mgL^{-1}$. From Fig. 9, 0.070 g/L was seen as best dosage to the degradation of pollutant molecules. At < 0.070 g/L of catalyst dosage a medium rate of degradation was observed due to less number of catalyst particles are present to large number of dyes particles. Further at >0.070 g/L of catalyst dosage the rate decreases even though the more number of catalyst particles are accessible. This was reveals that on the enhancement of catalyst dosage penetration capability of visible light into solution is decreased because of turbidity [40]. So that rate of degradation was reduced.

### D. Effect of initial dye concentration:

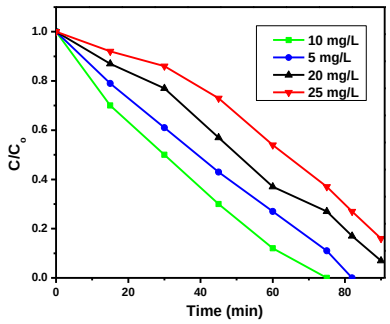


**Fig. 10. Effect of AR dye initial concentration at pH-4, NMT2 catalyst concentration 0.070 gL$^{-1}$**

This step was carried out at constant pH-4 and catalyst dosage 0.070 g/L by varying the AR dye concentration from 5 ppm to 25 ppm and the obtained reports are produced in Fig. 10. From the results it is found that up to 10 ppm, degradation considerably enhanced later on rate was diminished [41]. This can be clarified by associating with TEM and BET portrayal results. The diminished molecule size (6.5 nm) and high surface region (135.70 $m^2/g$) the rate of dye particles adsorbed on the surface of the impetus builds which supports the closeness with the •OH. It encourage the reaction between •OH and substrate atoms and prompts high rate of debasement of AR dye.

## V. CONCLUSIONS

In the current research work synthesized the $Mn^{2+}$and $Ni^{2+}$ co-doped $TiO_2$nanocatlysts (NMTs) by using sol-gel method. The photocatalytic activity of NMT2 is notable than compared to the remaining catalysts and undoped $TiO_2$, it was experimentally proved. By using various analytical techniques the photocatalysts were characterized. From the FT-IR technique it is proved that $Mn^{2+}$ and $Ni^{2+}$ were incorporated into crystal lattice of $TiO_2$. By this incorporation co-doped samples having the larger surface, smaller in size and less bandgap, which were confirmed by BET, XRD and UV-vis techniques respectively. Among all the prepared samples NMT2 (1.0 wt% $Ni^{2+}$ and 0.25 wt% $Mn^{2+}$) co-doped $TiO_2$ exhibited predominant photocatalytic activity compared to all other catalysts. It can be concluded that co-doping with transition metals is a promising route for enhanced photocatalytic degradation of pollutants.

## REFERENCES

1. S. Chatterjee, M.W. Lee and S.H. Woo, Adsorptive removal of Congo red, a carcinogenic textile dye by chitosan hydrobeads: binding mechanism equilibrium and kinetics, Colloids Surf. A. 2007, vol. 229, pp.146–152.
2. Z. Aksu, Application of biosorption for the removal of organic pollutants: a review, Process Biochem. 2005, vol. 40 (3), pp. 997–1026.
3. V. Gupta, I. Ali and D. Mohan, Equilibrium uptake and sorption dynamics for the removal of a basic dye (basic red) using low-cost adsorbents, J. Colloids Interface Sci. 2003, vol. 265 (2), pp. 257–264.
4. L. Wang, J. Zhang and A. Wang, Removal of methylene blue from aqueous solution using chitosan-g-poly (acrylic acid)/montmorillonite super adsorbent nanocomposite, Coll. Surf. A. 2008, vol. 322, pp. 47–53.
5. M. Farbob and E. Jafarpoor, Fabrication of different ZnO nanostructures and investigation of morphology dependence of their photocatalytic properties, Mater. Lett. 2012, vol. 85, pp. 47–49.
6. *V.Binas, D. Venieri, D. Kotzias and G. Kiriakidis, Modified $TiO_2$ based photocatalysts for improved air and health quality, J. Mater. 2017, vol. 3, pp. 3-16.*
7. S. S. Muniandy, N. H. MohdKaus, B. Zhong Tao Jiang, C. Mohammed noor Altarawnehc and H. Ling Lee, Green synthesis of mesoporous anatase $TiO_2$ nanoparticles and their photocatalytic activities, RSC Adv. 2017, vol.7, pp. 48083-90.
8. V.D.Binas, K.Sambani, T.Maggos, A.Katsanaki and G.Kiriakidis, Synthesis and photocatalytic activity of Mn-doped $TiO_2$ nanostructured powders under UV and visible light, A. catal. B: Environ. 2012, vol. 113–114, pp. 79-86.
9. N.T. Yong, L.W. Chung and R.M. Abdul, An Overview on the photocatalytic Activity of Nano-Doped-$TiO_2$ in the degradation of Organic Pollutants, ISRN Mater. Sci. 2011, pp.1-18.
10. S. Noor Begum, H. M. Farveez Ahmed and K. R. Gunashekar, Effects of Ni doping on photocatalytic activity of $TiO_2$thin films prepared by liquid phase deposition technique, B. Mater.Sci. 2008, vol. 31, pp. 747–751.
11. Y. Fei Zhao, L. Can, L.Song, R. Xi Liu, J. Yuan Hu, Y. Yan Gong and L. Yuan Niu, Electronic, optical and photocatalytic behavior of Mn, N doped and co-doped $TiO_2$: Experiment and simulation, J. S. State. Chem. 2016, vol. 235, pp. 160–168.
12. K. Umar AzmiAris, H. Ahmad, T.Parveen, J. Jaafar, Z. Abdul Majid, A.V. Bhaskar and J. Talib, Synthesis of visible light active doped $TiO_2$ for the degradation of organic pollutants-methylene blue and glyphosate, J. Anal. Sci .Tech. 2016, vol.7, pp. 20-29.
13. *D. Jing, Y. ZhangandL. Guo,Study on the synthesis of Ni doped mesoporous $TiO_2$ and its photocatalytic activity for hydrogen evolution in aqueous methanol solution,Chem. Phy. Letter. 2005, vol. 415, pp. 74-78.*
14. M. pelaez, I. Nicholas and T. T. Nolan, Environmental engineering and science program, school of energy, Environmental, Biological, and Medical engineering, university of cincinnati, cincinnati, ohio. 45221-0071, USA.
15. C. Shifu, Z. Sujuan and L. Wei, Z. Wei, Preparation and activity evaluation of p–n junction photocatalystNiO/$TiO_2$, J. Hazard.Mate. 2008, vol. 55, pp. 320–326.
16. K. Wilke and H. D. Breuer, The influence of transition metal doping on the physical and photocatalytic properties of titania, Int. J. Photoenergy. J. Photochem. Photobiol.A: Chemistry. 1999, vol. 121, pp. 49–53.
17. A. Tavakoli & Sohrabi, Morteza & Kargari and Ali, A Review of Methods for Synthesis of Nanostructured Metals with Emphasis on Iron Compounds. Chemical Papers. 2007, vol.61, pp. 151-170.
18. M. Manzoor A. Rafiq, M. Ikram, M. Nafees, S. Ali, Structural, optical and magnetic study of Ni-doped $TiO_2$ nanoparticles synthesized by sol–gel method, International Nano Letters, 2018, vol.8, pp. 1–8.
19. M.A. Salem, F.A. Ahmed and B.Z. Ahmed, Photo catalytic degradation of Allura red and Quinoline yellow with poly aniline/ $TiO_2$ nanocomposite, A.Catal. B: Environ. 2009, vol. 91, pp. 59-66.
20. B.K. Avasarala, T. Siva Rao and S. Bojja, Enhanced photocatalytic activity of beryllium doped titania in visible light on the degradation of methyl orange dye, Int. J. Mater. Res. 2010, vol. 101, pp. 1–7.
21. S. Abdul Alim, T. Siva Rao, I. Manga Raju, M. Ravi Kumar and K.V. Divya Lakshmi, Fabrication of visible light driven nano structured Copper, Boron co-doped $TiO_2$ for photocatalytic removal of Lissamine Green B, J. Sau. Chem. Soc. 2019, vol. 23, pp. 92-103.
22. J.C.S. Wu and C.H. Chen, A visible light responsive vanadium doped Titania nanocatalyst by sol-gel method. J. Photochem. Photobiol. A: Chem. 2014, vol. 163, pp 509-515.
23. N. Wetchakun, B. Incessungvorn, K. Wetchakun and S. Phanichphant, Influence of calcination temperature on anatase to rutile phase transformation in $TiO_2$ nanoparticles synthesized by the modified sol–gel method, Mater. Lett. 2012, vol. 82, pp.195–198.
24. E. Gharibshahi and E. Saion, Influence of Dose on particle size and optical properties of colloidal Platinum Nanoparticles. Inter.J.Mol. Sci. 2012, vol. 13, pp. 14723-14741.
25. K.Taranjeet , S. Abhishek , T. Amrit Pal and R.K. Wanchoo, Utilization of solar energy for the degradation of carbendazim and propiconazole by Fe doped $TiO_2$., Solar. Energy. 2016, vol. 125, pp. 65–76.
26. Y. Zhongping, J. Fanghou, T. Shujun, C. Xiang, J. Zhaohua and B. Xuefeng, Microporous Ni-doped $TiO_2$ film photocatalyst by plasma electrolytic oxidation, Appl. Mater. Sci. 2010, vol. 2, pp. 2617-2622.

27. N. Sharotri and D. Sud, A greener approach to synthesize visible light responsive nanoporous S-doped $TiO_2$ with enhanced photocatalytic activity. New J. Chem. 2015, vol. 39, pp. 217-223.
28. I. Othmana, R.M. Mohamed and F.M. Ibrahem, Study of photocatalytic oxidation of indigo carmine dye on Mn-supported $TiO_2$, J. Photochem. Photobiol A: Chemistry. 2007, vol. 189, pp. 80–85.
29. S. JENSEN AND S.D. KILIN, ELECTRONIC PROPERTIES OF NICKEL-DOPED $TiO_2$ANATASE, J. PHY. COND. MAT. 2015, VOL. 27, PP. 1 13.
30. S. MUNIR SHAH AND S.M.H. HUSSAIN, EFFECT OF CARRIER CONCENTRATION ON THE OPTICAL BAND GAP OF $TiO_2$ NANOPARTICLES, MATER. DES. 2016, VOL. 92 , PP. 64–72.
31. Y. Wang, R. Zhang., Jianbao, Li. Liangliang and Li. Shiwei Lin, First principles study on transition metal-doped anatase $TiO_2$, Nano scale Res. Lett. 2014, vol. 9, pp. 35-46.
32. S.Chang, H. Chien-yao, L.Pin-han and T. Chang, Preparation of phosphate Zr doped TiO2 exhibiting high photocatalytic activity through calcination of ligand-capped nanocrystals. Appl. catal B: Environ. 2009, vol. 90, pp. 233-241.
33. D. Christian , A. Miguel Pérez-Osorio, S. Christopher Kley, P.Punke, E. Christopher Patrick, P. Jacobson, F.Giustino, S. Jung Jung, and K. Kern,$TiO_2$ Anatase with a Bandgap in the Visible Region, *Nano Lett.* 2014, vol. 14, pp. 6533–6538.
34. R. Chauhan., A. Kumar and R. Pal Chaudhary, Structural and photocatalytic studies ofMn doped TiO2 nano particles, Spectro.chem. act. part A: molecule. Biomolecule. Spec. 2012, vol. 98, pp. 256-264.
35. V. Bhatia and A. Dhir, Transition metal doped $TiO_2$ mediated photocatalytic degradation of anti-inflammatory drug under solar irradiations, J. Environ. Chem. Eng. 2016, vol.4, pp. 1267–1273.
36. H. Huang, R. Cao, S. Yu, K. Xu, W. Hao, Y. Wang, F. Dong, T. Zhang and Y. Zhang, Single-unit-cell layer established Bi2WO6 3D hierarchical architectures: efficient adsorption, photocatalysis and dye sensitized photoelectrochemical performance, Appl. Catal. B. 2017, vol. 219, pp. 526–537.
37. G. Zeng, J. Wan, D. Huang, L. Hu, C. Huang, M. Cheng, W. Xue, X. Gong, R. Wang and D. Jiang, Precipitation, adsorption and rhizosphere effect: the mechanisms for Phosphate-induced Pb immobilization in soils-A review, J. Hazard Mater. 2017, vol. 339, pp. 354–367.
38. K. Wang, Y.Hisieh, C.Wu and C. Chang, The pH and anion effects on the heterogeneous photocatalytic degradation of o-methyl benzoic acid in $TiO_2$ aqueous suspension, Chemosphere . 2000, vol. 40, pp. 389-97.
39. M.A. Rauf and S. Salman Ashraf, Fundamental principles and application of heterogeneous photocatalytic degradation of dyes in solution. Chem. Eng. J. 2009, vol. 5, pp. 10–18.
40. N. Venkatachalam, M. Palanichamy and V. Murugesan, Sol-gel preparation and characterization of alkaline-earth metal doped nano $TiO_2$: efficient photocatalytic degradation of 4-chlorophenol, J. Mol. Catal. A; Chem. 2007, vol. 273, pp. 177–185.
41. C.H. Chiou and R. S. Juang, Photocatalytic degradation of phenol in aqueous solutions by Pr-doped $TiO_2$ nanoparticles, J. Hazard. Mater. 2007, vol. 149, pp. 669-678.


## AUTHORS PROFILE

**Mr. Sankara Rao Miditana** has been working as Lecturer in Chemistry at STSN Government Degree College, Kadiri, Andhra Pradesh is currently pursuing Ph.D degree in Chemistry at Andhra University, Visakhapatnam, India. His research interests are synthesis, Characterization and Photocatalytic applications of $TiO_2$ based nanomaterials.

**Prof. T. Siva Rao** is an Professor and Research Director, Dept. of Inorganic & Analytical Chemistry, A.U. College of Science & Technology, Andhra University. 25 Ph.D. and 5 M.Phil. degrees are awarded under his supervision. Published 125 Research Articles in International Journals and completed 4 National Projects. Life member, Indian Science Congress Association, Life member, Catalysis Society of India, IIT – Madras, Member, Indian Chemical Society, Kolkata. Area of research is Heterogeneous Phtocatalysis, Organic – Inorganic nano hybrid materials, Redox Flow Batteries, Bio adsorption of Pollutants.

**Dr. Shaik Abdul Alim**, M.Sc., Ph.D. A.U. College of Science & Technology, School of Chemistry, Andhra University, Visakhapatnam. Published 5 Research Articles in the reputed peer reviewed International Journals. Field of Research $TiO_2$ nano materials, Heterogeneous Phtocatalysis, Organic – Inorganic Nano hybrid materials, Bio adsorption of Pollutants, Published my first Research Article in Journal of Saudi Chemical Society, title "Fabrication of visible light driven nano structuredCopper, Boron codoped $TiO_2$ for photocatalyticremoval of Lissamine Green B", Poster Presented at International Conference SUCHEM 2018, $5^{th}$ – $8^{th}$ August, 2018, CSIR-Indian Institute of Chemical Technology, Hyderabad (Telangana State) India – 500007.

**Mr. Imandi Manga Raju** is a post graduate in Chemistry. Now he is pursuing his Ph.D in Chemistry at Andhra University, Visakhapatnam, India.. He is currently working on synthesis, characterization and applications of $TiO_2$ based nanomaterials for photocatalytic degradation of organic pollutants and pathogens from polluted waste water and published 7 research articles in reputed peer reviewed Elsevier and Springer journals.